Thermochimica Acta, 117 (1987) 201–217
Elsevier Science Publishers B.V., Amsterdam – Printed in The Netherlands

THERMOANALYTICAL STUDIES OF ZINC CITRATE, BISMUTH CITRATE AND CALCIUM CITRATE *

A. SRIVASTAVA, V.G. GUNJIKAR ** and A.P.B. SINHA
Physical Chemistry Division, National Chemical Laboratory, Pune (India)
(Received 6 January 1987)

ABSTRACT

Thermal decomposition behaviour of the citrates of zinc, bismuth and calcium has been investigated individually and as binary mixtures (1:1) consisting of zinc citrate as the essential component. Zinc citrate is found to decompose to zinc oxide at 400 °C, bismuth citrate decomposes to α-Bi_2O_3 at 360 °C and calcium citrate decomposes to calcium oxide at 1150 °C. The barium and calcium oxides which are normally formed at a higher temperature during the individual decomposition of the citrates are obtained at lower temperatures, i.e. 1140 and 800 °C, respectively, on decomposition of their mixtures with zinc citrate. Bismuth citrate alone is found to decompose to α-Bi_2O_3 whereas its mixture with zinc citrate decomposes to the β-phase of bismuth oxide.

INTRODUCTION

The usual method of preparing oxide compositions for electronic ceramics consists of grinding or milling the oxides or carbonates and sintering them at high temperatures to obtain the desired product. Since electronic ceramics require precise control of stoichiometry and reproducibility to achieve the desired electrical properties, some non-conventional solution methods of preparation could be of advantage in obtaining homogeneous mixtures of oxides. In the present work some zinc oxide-based electronic ceramics which show deviation from Ohm's law giving rise to non-linear current–voltage characteristics and which find application as voltage surge absorbers have been prepared by a novel non-conventional preparation technique known as the liquid mix technique [1,2]. These electroceramics consist of zinc oxide [3] as the major component and one or more additive oxides in smaller concentrations which are responsible for the non-linear behaviour. The additive oxides used in the present study are Bi_2O_3, BaO and CaO. These

* NCL communication No. 4189.
** To whom all correspondence should be addressed.

0040-6031/87/$03.50

oxides are required to be uniformly dispersed in the base material in order to obtain good non-linearity. Therefore, a liquid mix technique which gives mixing at the atomic level has been used to obtain homogeneous mixtures of the oxides. This technique involves the formation of citrates of the metals which on decomposition give rise to the oxides. In order to identify the temperature of decomposition of the organic material, the temperature of formation of the oxides as well as the probable intermediates obtained during the various stages of decomposition, it was considered appropriate to study the thermal decomposition of the citrates of zinc, bismuth and calcium systematically. The thermal decomposition of barium citrate has already been reported [4]. The decomposition study of the binary mixtures of citrates of zinc and barium, zinc and bismuth and zinc and calcium has also been included. A review of the literature [5–7] revealed little information on the decomposition behaviour of these citrates and hence a systematic study of the thermal decomposition of these citrates individually, and as admixtures was undertaken in the present work.

EXPERIMENTAL

Preparation

The citrates of zinc, bismuth and calcium were prepared by reacting zinc chloride (May and Baker, LR grade), bismuth nitrate (BDH, AR grade) respectively with sodium citrate (Merck, AR grade). Each of these salts and sodium citrate were accurately weighed in the required stoichiometric proportion. Saturated solutions of each were prepared in distilled water. To each solution a saturated solution of sodium citrate was added with constant stirring. The reaction resulted in the formation of the respective citrates as precipitates which were filtered off, dried in low vacuum and used for thermal studies.

Binary mixtures of zinc citrate and barium citrate, zinc citrate and bismuth citrate and zinc citrate and calcium citrate were prepared by accurately weighing the individual citrates in mole ratio and grinding together in an agate mortar for one hour. The mixtures thus obtained were used for thermal analysis.

Instrumental

A Netz'ch STA 409 differential thermal analyser was used to obtain the thermal data on the citrates. The thermal analyser simultaneously plots the results of differential thermal analysis (DTA), thermogravimetric analysis (TGA) and derivative thermogravimetric analysis (DTG) along with the sample temperature (T). For the analysis, 50 mg of the sample were placed

in a cylindrical-type platinum crucible mounted on one of the 2 mm alumina rods of the sample carrier covering the Pt/Pt–10% Rh differential thermocouple which can measure the sample temperature simultaneously. The sample was heated in dynamic air atmosphere at a rate of 10 °C min^{-1}. A chart speed of 120 mm h^{-1} was used during the thermogravimetric scan.

To support the thermogravimetric data, infrared (IR) spectra of the original sample and intermediate compounds were recorded in nujol on a Pye Unicam IR Spectrometer (SP3-300).

RESULTS AND DISCUSSION

Thermal decomposition of zinc citrate

Zinc citrate [$Zn_3(C_6H_5O_7)_2$], when heated in dynamic air atmosphere at a rate of 10 °C min^{-1}, showed that its decomposition to zinc oxide is a 3-step process. The TG, DTG and DTA curves together with the sample temperature are shown in Fig. 1. The weight losses obtained at various stages of decomposition are summarized in Table 1.

The IR spectrum recorded for zinc citrate is shown in Fig. 2. As can be seen in the spectrum, the zinc citrate does not appear to contain water of crystallization prepared since the hydroxyl band observed at 3460 cm^{-1} is

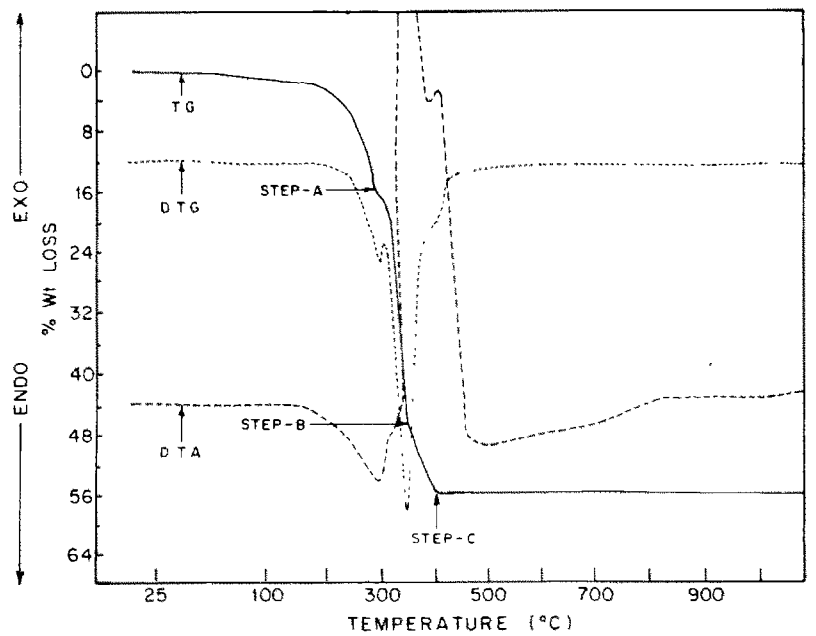

Fig. 1. TG, DTG and DTA curves of zinc citrate in air.

TABLE 1

Thermal analysis data for the decomposition of zinc citrate

Decomposition step	% Wt. loss observed at the end of each step	% Wt. loss calculated	Temp. range (°C)	Peak temp (°C)	Type of reaction
A	16.2	16.0	25–305	301	Endothermic
B	32.5	32.6	305–388	353	Exothermic
C	9.0	8.9	388–418	400	Exothermic

quite sharp unlike the broad band usually observed for the weakly bonded –OH groups. This is also confirmed by the DTG analysis which shows no peak characteristic of the loss of absorbed water. The sharp –OH stretching band is, therefore, due to the –OH group incorporated in the citrate molecule. The IR spectrum (Fig. 2) of the sample obtained after the first step (Step A) of decomposition in the temperature range 25–305 °C shows a reduction in the intensities of the citrate bands compared to that of the original sample. The sharp –OH band observed in the IR spectrum of the original sample has now disappeared. This clearly shows loss of the –OH group from the citrate molecule. The reduction in the intensities of the

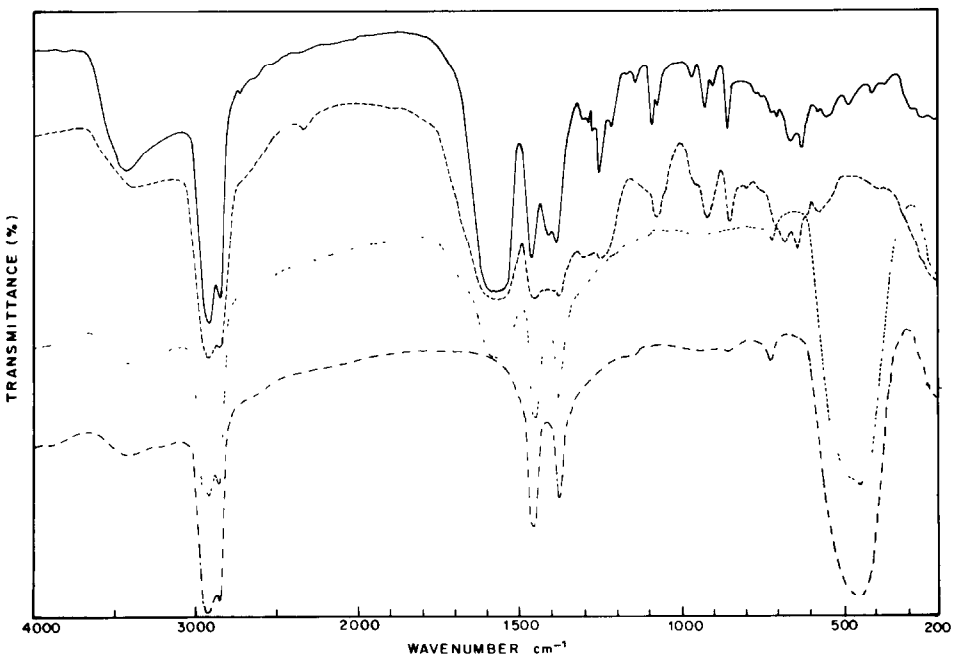

Fig. 2. IR spectra of zinc citrate (———), decomposition steps A (- - - - - -), B (· · · · · ·) and C (· – · – · –).

citrate bands is indicative of the partial decomposition of the citrate. The intensity of the carboxylate band at 1580 cm^{-1} is lowered to two-thirds of that present in the original citrate. There is no indication of unsaturation i.e. the presence of $\diagup C{=}C \diagdown$ bands in the IR spectrum at this stage. The spectrum does not show the presence of zinc carbonate or ZnO bond formation. As the reaction during this stage is observed to be endothermic, there is no burning of carbon with the outside oxygen and, therefore, the weight loss during this step can be attributed to the loss of two molecules of water and carbon monoxide from the citrate moiety leading to the formation of the intermediate as shown in the decomposition scheme. The possibility of the formation of oxalate is also remote as the X-ray diffraction pattern recorded for the sample obtained at the end of this stage did not match that reported for zinc oxalate. The loss due to H_2O and CO removal (16.0%) is in agreement with that experimentally observed (16.2%) for this step.

The IR spectrum (Fig. 2) of the sample obtained at the end of the second stage (Step B) which is exothermic, as indicated by the DTA curve in the temperature range 305–388 °C shows almost complete reduction in the intensity of the citrate bands except the carboxylate band which appears at 1580 cm^{-1} but with reduced intensity. The spectrum shows the appearance of a new, strong band in the low frequency region of the spectrum. This strong band at 450 cm^{-1} is found to correspond to zinc oxide [8]. Thus, it is presumed that at this stage the citrate has further decomposed forming zinc oxide and $Zn(CH_3COO)_2$ (Scheme 1). The presence of $-CH_3$ groups was found by recording an IR spectrum of the sample obtained at the end of this stage in HCB instead of nujol. The spectrum showed a $-CH_3$ stretching absorption at 930 cm^{-1} and a symmetric deformation absorption at 1385 cm^{-1}. The experimental weight loss of 32.5% in this step is in agreement with the calculated loss.

The IR spectrum (Fig. 2) of the sample obtained at the end of the third stage (Step C) of decomposition which is exothermic, in the temperature range 388–418 °C, shows complete absence of the bands due to citrate and the presence of the strong zinc oxide band at 450 cm^{-1} only. Thus, at the end of this stage the citrate has decomposed completely to zinc oxide. The observed weight loss of 9% for this step agrees with the calculated loss of 8.9% for the formation of zinc oxide.

$$2Zn_3(C_6H_5O_7)_2 \xrightarrow[\substack{-4H_2O \\ -4C(\text{as CO}) \\ -4O}]{25\text{–}305\,^\circ C} 2Zn_3(C_4H_3O_5)_2 + 4C \qquad (1)$$

$$2Zn_3(C_4H_3O_5)_2 \xrightarrow[\substack{-12C(\text{as CO, } CO_2) \\ -6H \\ -11O}]{305\text{–}385\,^\circ C} 5ZnO + Zn(CH_3COO)_2 \qquad (2)$$

$$Zn(CH_3COO)_2 \xrightarrow[\substack{-4C(\text{as CO, } CO_2) \\ -3O \\ -3H}]{388\text{–}418\,^\circ C} ZnO \qquad (3)$$

Scheme 1. Decomposition scheme of zinc citrate.

Since the IR spectra at any stage of decomposition has no new bands other than those for zinc oxide, the decomposition of zinc citrate appears to be a gradual burning process resulting finally in the formation of zinc oxide at 400 °C.

Thermal decomposition of bismuth citrate

The thermogravimetric spectrum recorded for bismuth citrate $[Bi(C_6H_5O_7) \cdot H_2O]$ in dynamic air heated at a rate of 10 °C min^{-1} is shown in Fig. 3 with the DTG and DTA curves. It is evident from the spectrum that decomposition of bismuth citrate to bismuth oxide involves three steps. The weight losses obtained at various stages of the decomposition process are given in Table 2.

The first step (Step A) of the TG curve in the temperature range 25–225 °C is endothermic indicating dehydration of the citrate at this stage. The dehydration begins at 39 °C and is completed by 225 °C. The IR spectrum (Fig. 4) of the sample obtained at the end of this stage shows a sharp band at 3470 cm^{-1} as against a broad band observed in the IR spectrum of the original citrate shown in Fig. 4. This indicates the loss of the weakly-bonded water of crystallization at the end of this stage. With the removal of this water the IR spectrum also showed sharpening of the citrate bands compared with those observed in the spectrum of the original citrate.

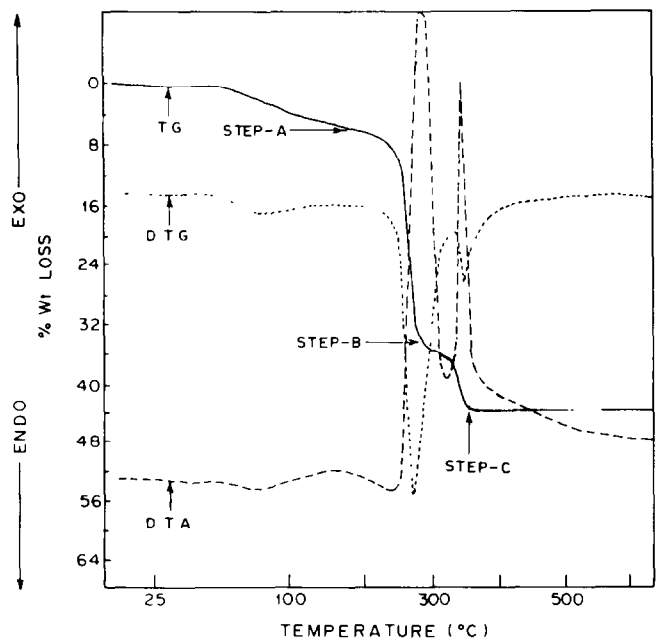

Fig. 3. TG, DTG and DTA curves of bismuth citrate in air.

TABLE 2

Thermal analysis data for the decomposition of bismuth citrate

Decomposition step	% Wt. loss observed at the end of each step	% Wt. loss calculated	Temp. range (°C)	Peak temp. (°C)	Type of reaction
A	5.29	5.35	25–225	77	Endothermic
B	29.30	30.20	225–332	274	Exothermic
C	9.10	9.00	332–410	350	Exothermic

The weight loss observed for this stage (5.29%) tallies with the calculated loss of 5.35% for the removal of about one mole of the absorbed water.

The IR spectrum (Fig. 4) of the product obtained at the end of the second exothermic stage of decomposition (Step B) in the temperature range 225–332°C showed a considerable reduction in the intensities of the citrate bands with the carboxylate band still appearing at 1550 cm^{-1}. The hydroxyl

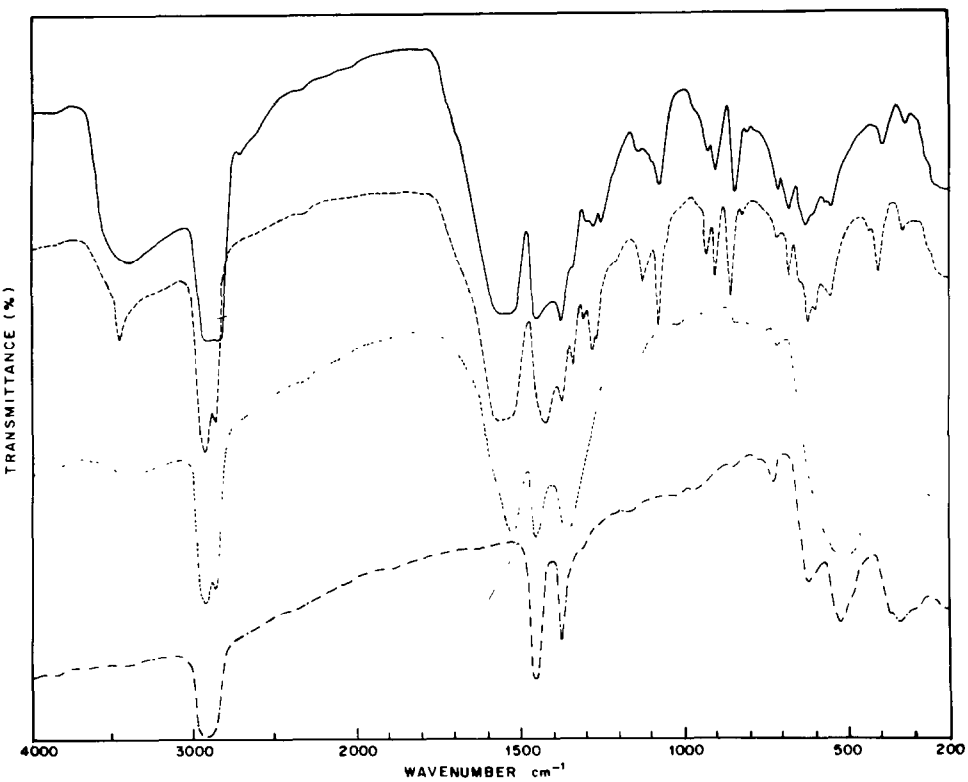

Fig. 4. IR spectra of bismuth citrate (———), decomposition steps A (- - - - - -), B (· · · · · ·), C (· – · – · –).

$$4BiC_6H_5O_7 \cdot H_2O \xrightarrow[-H_2O]{25-225\,^\circ C} 4BiC_6H_5O_7 \quad (1)$$

$$4BiC_6H_5O_7 \xrightarrow[\substack{-18C(\text{as CO, } CO_2)\\ -11H\\ -17\,5O}]{225-332\,^\circ C} 3[BiO(CH_3COO)] + \tfrac{1}{2}Bi_2O_3 \quad (2)$$

$$3[BiO(CH_3COO)] \xrightarrow[\substack{-6C(\text{as CO, } CO_2)\\ -9H\\ -4\,5O}]{332-410\,^\circ C} 3/2Bi_2O_3 \quad (3)$$

Scheme 2. Decomposition scheme of bismuth citrate.

stretching band at 3470 cm^{-1} was found to be absent at this stage indicating loss of the –OH group from the citrate molecule. New bands were observed in the oxide region of the IR spectrum. These bands which appeared at 645(w), 505(s) and 345(s) cm^{-1} were found to correspond to the α-phase of Bi_2O_3 [9]. Thus, the citrate at this stage has decomposed partially, giving rise to Bi_2O_3 and $BiO(CH_3COO)$ as shown in the decomposition scheme (Scheme 2). The presence of $-CH_3$ was shown in an IR spectrum of the sample obtained at the end of this stage in HCB. The spectrum showed the presence of the $-CH_3$ stretching frequency at 2940 cm^{-1} and symmetric deformation absorption at 1410 cm^{-1}. The observed weight loss of 29.3% for this step agrees fairly well with the calculated loss of 30.2%.

In the third decomposition step (Step C), in the temperature range 332–410 °C, further decomposition of the intermediate takes place. No bands due to citrate were observed in the IR spectrum (Fig. 4) for this stage. The oxide bands obtained in the spectrum are now much stronger, possibly because of the complete formation of Bi_2O_3 at the end of this stage. The weight loss (9.1%) observed during this step agrees with the calculated loss of 9.0% for the complete formation of Bi_2O_3.

Thus, the thermal decomposition of bismuth citrate is also a gradual burning process leading directly to the formation of α-Bi_2O_3 at 350 °C. No new bands, except for the oxide bands, were observed in the IR spectra at any stage of decomposition.

Radecki et al. [6] have reported a three-step scheme for the decomposition of bismuth citrate in which there is no loss in weight up to 100 °C. Loss of water from the citrate takes place at 470 °C and Bi_2O_3 is formed at 740 °C. Our study, however, shows the loss of H_2O at about 225 °C and total breakdown of the sample to Bi_2O_3 at about 410 °C.

Thermal decomposition of calcium citrate

The derivatograph of calcium citrate is shown in Fig. 5. The endotherm and exotherm observed in the differential thermal analysis curve with its temperature range and corresponding weight loss in thermogravimetry at the final temperature and successive decomposition steps in differential thermo-

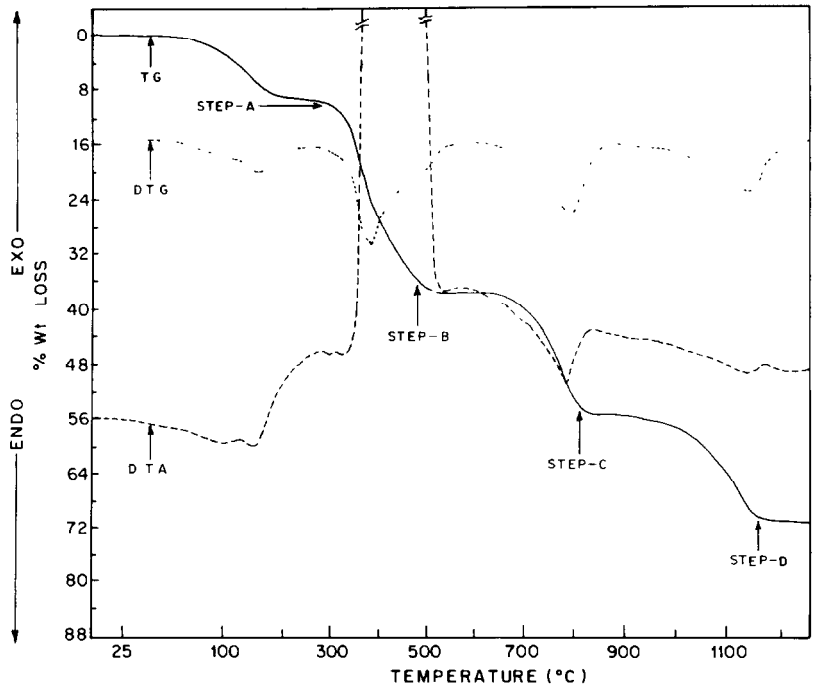

Fig. 5. TG, DTG and DTA curves of calcium citrate in air.

gravimetry are given in Table 3. As shown in the figure, the decomposition of calcium citrate carried out at a rate of 10 °C min^{-1} is a four-step process.

The first step (Step A) of the TG curve in the temperature range 25–240 °C shows an endothermic change corresponding to dehydration. This dehydration step is divided into two parts. The first part, in the temperature range 25–141 °C with the weight loss of 3.2% corresponds to the loss of one molecule of the absorbed water while the second part in the temperature range 141–240 °C with a weight loss of 6.2% corresponds to the loss of two molecules of absorbed water. The total weight loss of 9.4%

TABLE 3

Thermal analysis data for the decomposition of calcium citrate

Decomposition step	% Wt. loss observed at the end of each step	% Wt. loss calculated	Temp. range (°C)	Peak temp. (°C)	Type of reaction
A	9.4	9.5	25–240	170	Endothermic
B	28.2	28.4	240–542	395	Exothermic
C	17.5	17.2	542–870	795	Endothermic
D	15.9	15.5	870–1210	1150	Endothermic

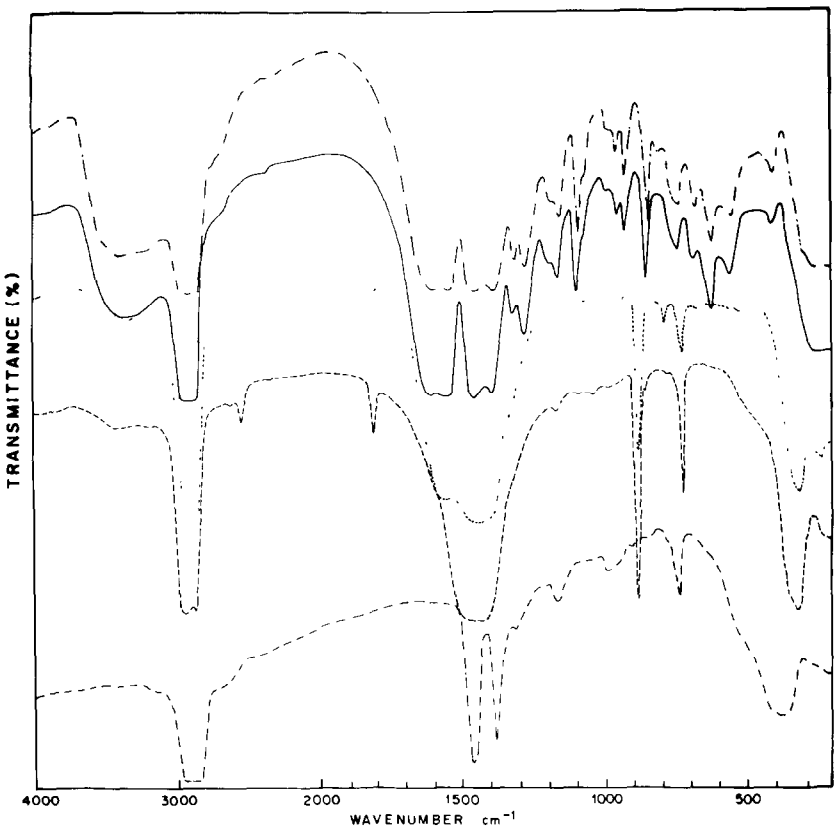

Fig. 6. IR spectra of calcium citrate (– · · – · · –), decomposition steps A (———), B (· · · · · ·), C (- - - - - -) and D (· – · – ·).

observed at the end of the first step is in agreement with the loss of 3 moles of crystalline water (amounting to 9.5% of the total weight of the citrate). The dehydration starts at 32.5 °C and is completed at 240 °C. The IR spectrum (Fig. 6) recorded for the sample obtained at the end of this stage shows a reduction in the broad hydroxyl band intensity at 3400 cm^{-1} compared with that observed in the IR spectrum of the original citrate (Fig. 6).

The IR spectrum of the sample obtained at the end of the second decomposition step (Step B) in the temperature range 240–342 °C (Fig. 6) shows the absence of the hydroxyl band at 3400 cm^{-1} indicating the completion of dehydration of the citrate. The spectrum also shows the appearance of some new and strong bands at 2540(w), 1800(w), 1450(vvs), 875(vs), 720(ms) and 320(vs) cm^{-1}, which are similar to those of calcium carbonate [10]. Another new medium strong band appearing at 790 cm^{-1} can be ascribed to the –CH out-of-plane deformation mode of the $R_1CH{=}CR_2R_3$ group [11]. As observed in the spectrum, there is a consider-

$$Ca_3(C_6H_5O_7)_2 \cdot 4H_2O \xrightarrow[-H_2O]{25-141\,^\circ C} Ca_3(C_6H_5O_7)_2 \cdot 3H_2O \quad (1a)$$

$$Ca_3(C_6H_5O_7)_2 \cdot 3H_2O \xrightarrow[-H_2O]{141-240\,^\circ C} Ca_3(C_6H_5O_7)_2 \cdot H_2O \quad (1b)$$

$$Ca_3(C_6H_5O_7)_2 \cdot H_2O \xrightarrow[\substack{-3H_2O \\ -6C(CO,\,CO_2) \\ -4H \\ -2O}]{240-542\,^\circ C} 1/3(Ca_3[(COO)CH{=}C(COO)CH_2(COO)]_2 \quad (2)$$

$$1/3(Ca_3[(COO)CH{=}C(COO)CH_2(COO)]_2) \xrightarrow[\substack{-4C(as\ CO,\,CO_2) \\ -3O \\ -2H}]{542-870\,^\circ C} 2CaCO_3 + CaO \quad (3)$$

$$2CaCO_3 \xrightarrow[-2CO_2]{870-1210\,^\circ C} 2CaO \quad (4)$$

Scheme 3. Decomposition scheme of calcium citrate.

able reduction in the intensities of the citrate bands. Therefore, at the end of this exothermic stage, decomposition of the citrate takes place giving calcium carbonate and aconitic acid as shown in Scheme 3. Formation of a little aconitic acid during the pyrolysis of calcium citrate has also been reported by Smeets [7]. The observed weight loss of 28.2% obtained during this stage is in agreement with the calculated loss of 28.4%.

The IR spectrum recorded for the sample obtained at the end of the third stage (Step C) which is endothermic, in the temperature range 542–870 °C is shown in Fig. 6. There is complete absence of the bands due to citrate. The spectrum shows bands corresponding to calcium carbonate and calcium oxide. The bands due to calcium oxide [12] are observed at 1160, 980, 520 and 385 cm^{-1}. Therefore, in this step, complete decomposition of the citrate has taken place and the weight loss observed can be attributed to the formation of two molecules of calcium carbonate and one molecule of calcium oxide as shown in the decomposition scheme. The observed weight loss at this stage was 17.1% which agrees with the calculated loss of 17.2%.

The IR spectrum of the material obtained after the fourth endothermic decomposition step (Step D) of the TG curve in the temperature range 870–1210 °C is also shown in Fig. 6. Only the bands corresponding to calcium oxide are observed in the Figure and the carbonate bands observed in the previous spectrum are absent at this stage. This shows that calcium carbonate has decomposed totally to calcium oxide during this stage. The weight loss of 15.9% observed during this stage agrees fairly well with the calculated loss of 15.5% for the formation of calcium oxide.

Thermal decomposition of a mixture (1 : 1) of zinc citrate and barium citrate

A thermogravimetric scan of a mixture of zinc and barium citrates in mole ratio is shown in Fig. 7. The organic part of the mixture was found to decompose at a temperature of 460 °C (Step C of the TG curve) leaving a

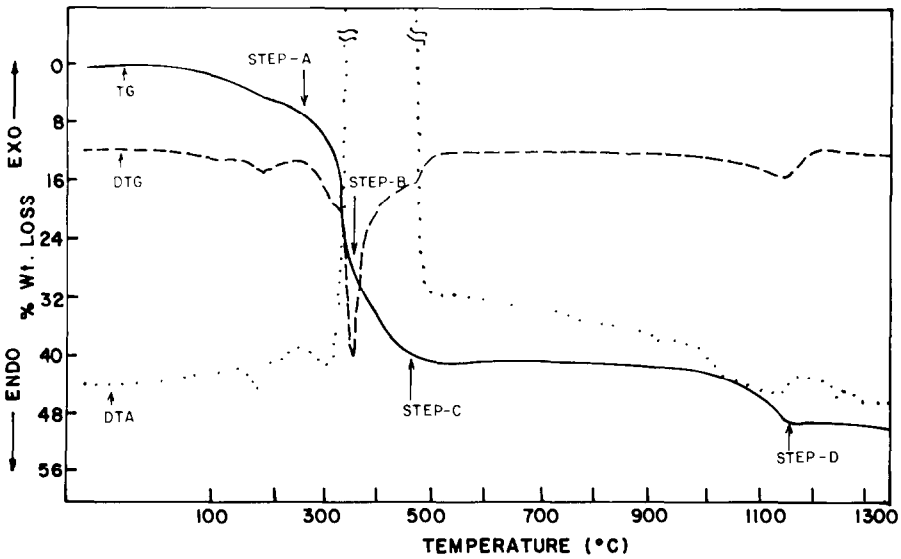

Fig. 7. TG, DTG and DTA curves of a mixture (1 : 1) of zinc citrate and barium citrate in air.

mixture of zinc oxide and barium carbonate. An IR spectrum (Fig. 8) recorded for the sample obtained at the end of this stage showed the presence of some bands at 2440(w), 1440(vvs), 1055(w), 860(s), 720(w) and 690(ms) cm^{-1}. These bands were found to compare with those of barium carbonate [10]. The strong band observed at 450 cm^{-1} corresponds to that of zinc oxide. The weight loss of 40.56% obtained in this stage agrees with the theoretical loss of 40.5% for the formation of ZnO and $BaCO_3$. The TG

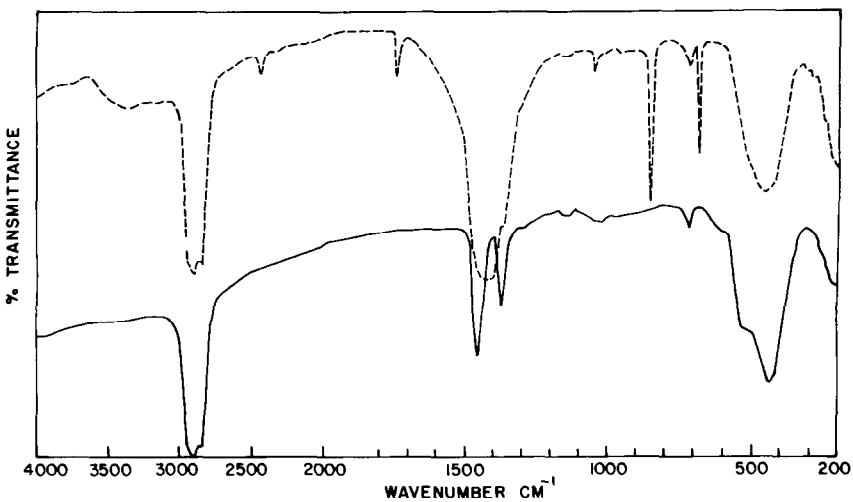

Fig. 8. IR spectra of decomposition steps C (- - - - - -) and D (———) of zinc citrate + barium citrate (1 : 1) mixture.

curve shows that this step (Step C) is stable up to 875 °C after which further loss begins leading to the final step (Step D). $BaCO_3$, therefore, is stable up to 875 °C and thereafter loss of CO_2 takes place leading to the formation of zinc oxide and barium oxide.

The IR spectrum of the sample obtained at the end of stage D is shown in Fig. 8. This spectrum has only two strong bands at 530 and 440 cm^{-1} in the oxide region of the spectrum. No bands due either to barium carbonate or barium oxide are observed. The barium oxide bands have been reported to occur at 503(sh), 483(s), 305(sh), 283(m) and 255(m) cm^{-1} [9]. Since BaO is known to be unstable and cannot exist as such, it is possible that it reacts with zinc oxide forming some new compound, most likely barium zincate ($BaZnO_2$) as the zinc and barium citrates have been taken in 1 : 1 proportion.

This study shows that during the decomposition of the binary mixture of zinc and barium citrates, barium oxide is formed at about 1140 °C. Barium citrate heated alone is found to decompose to barium oxide at a temperature of about 1700 °C [13]. It can, therefore, be concluded that at lower temperatures reactive oxides could be obtained from the decomposition of the citrate mixture.

Thermal decomposition of a mixture of zinc citrate and bismuth citrate

The decomposition of this mixture takes place in three stages as shown in the thermogravimetric scan (Fig. 9).

An infrared spectrum (Fig. 10) recorded for the material obtained at 450 °C (Step C of the TG curve) shows absorption bands at 505, 440, 380 and 335 cm^{-1} in the oxide region of the IR spectrum. No bands due to citrate are observed in this spectrum. The band at 440 cm^{-1} belongs to zinc oxide. The other bands in the region do not correspond to bismuth carbonate and, hence, could be attributed to bismuth oxide. During the individual decomposition of bismuth citrate the end product was observed to be α-Bi_2O_3 which showed IR bands at 645(w), 505(s) and 345(s) cm^{-1}. These bands, however, are not observed in the present spectrum. It can, therefore, be concluded that a different form of Bi_2O_3 is probably formed during the decomposition of the mixture. This is shown to be the β-Bi_2O_3 phase by X-ray diffraction measurements [14]. A final loss of 49.9% observed at the end of step C of the TG curve agrees fairly well with the loss of 52.1% calculated for the formation of ZnO and Bi_2O_3. The loss in weight observed above 1040 °C could be due to evaporation of Bi_2O_3 from the sample.

Thermal decomposition of a mixture (1 : 1) of zinc citrate and calcium citrate

The thermogravimetric scan of a mixture of zinc citrate and calcium citrate in mole ratio is shown in Fig. 11. The DTG trace shows that the total

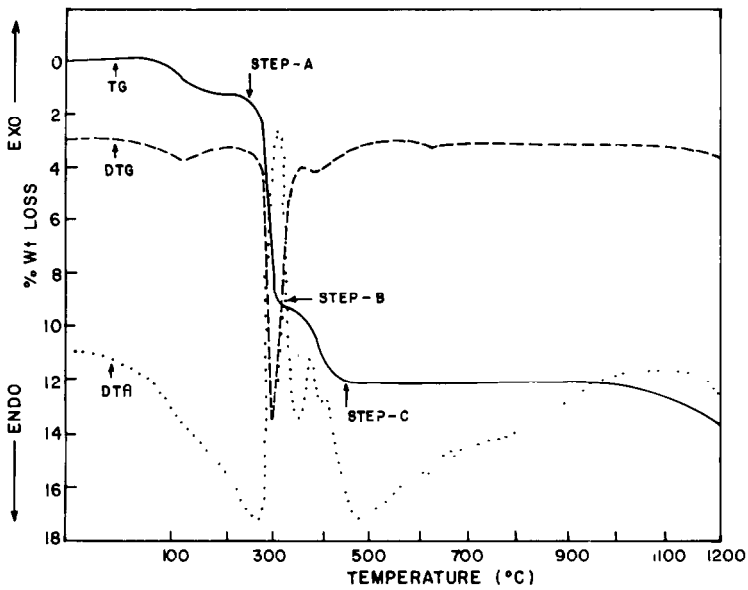

Fig. 9. TG, DTG and DTA curves of a mixture (1 : 1) of zinc citrate and bismuth citrate in air.

decomposition occurs in five steps. A total weight loss of 63.2% observed at the end of the decomposition process is in good agreement with the calculated loss of 64.07% for the formation of zinc oxide and calcium oxide. The citrate part of the mixture was found to decompose at 500 °C (Step C) giving rise to zinc oxide and calcium carbonate. The IR spectrum for the material obtained at the end of this stage is shown in Fig. 12. The spectrum shows absorption bands at 2500(w), 1790(w), 1440(vvs), 875(vs), 705(ms) and 310(vs) cm^{-1} which correspond to calcium carbonate, and a strong band at 450 cm^{-1} corresponding to zinc oxide. No bands due to citrate are observed in this spectrum. A weight loss of 47.03% was observed during this

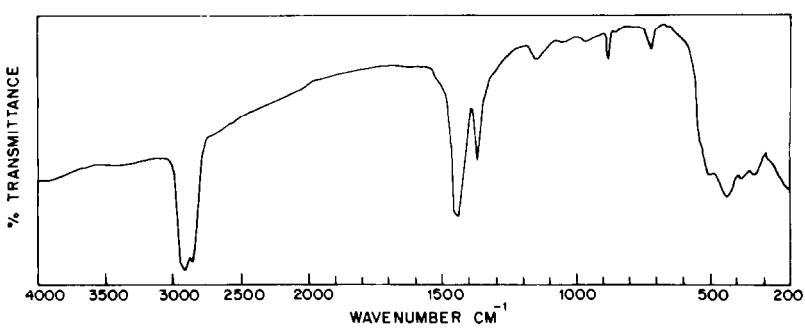

Fig. 10. IR spectrum of decomposition step C of zinc citrate + bismuth citrate (1 : 1) mixture.

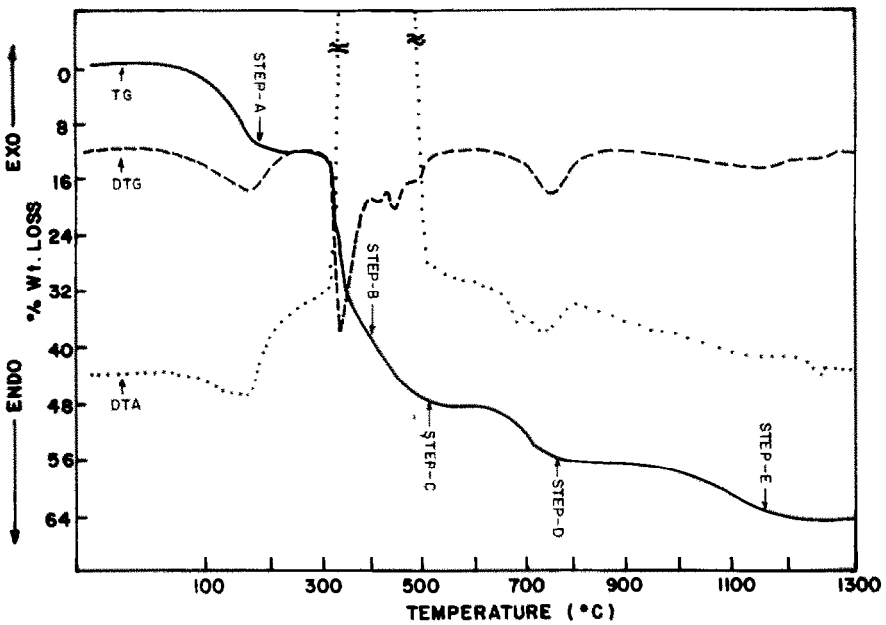

Fig. 11. DTG and DTA curves of a mixture (1 : 1) of zinc citrate and calcium citrate in air.

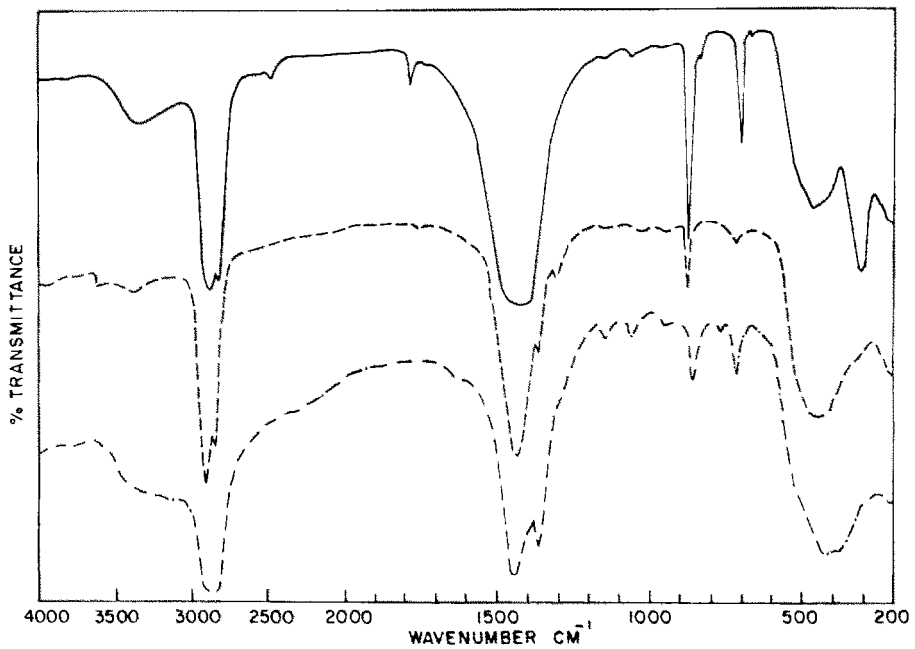

Fig. 12. IR spectra of decomposition steps C (———), D (- - - - - -) and E (· — · — ·) of the zinc citrate + calcium citrate (1 : 1) mixture.

stage. This loss, however, is less than the calculated loss of 52.5% required for the formation of ZnO and $CaCO_3$. This discrepancy could be attributed to unreacted carbon trapped within the residue.

The IR spectrum (Fig. 12) recorded for the sample left at the end of stage D at 787 °C showed no bands due to calcium carbonate. Only bands corresponding to CaO and ZnO are observed in the spectrum, indicating that $CaCO_3$ is completely decomposed to CaO in this endothermic stage. Further loss observed after this step may be attributed to the loss of CO or CO_2 from the sample. The IR spectrum recorded for the sample obtained at the end of stage E which is also endothermic is shown in Fig. 12. This spectrum is slightly different from that obtained at the end of stage D. This could be due to the reaction between ZnO and CaO resulting in the formation of some new compound, probably calcium zincate. Therefore, at 787 °C, ZnO and CaO exist as such whereas at higher temperatures (1200–1400 °C) they react together forming a new compound.

Thus, during the individual decomposition of calcium citrate, CaO is formed at about 1150 °C whereas during the decomposition of the mixture CaO is obtained at 800 °C.

CONCLUSIONS

(1) The mixtures of citrates and the oxides obtained from them were homogeneously mixed since no difference in behaviour was observed in different parts of the sample in thermogravimetric or infrared measurements.

(2) The residue obtained as a result of the thermal decomposition was purely crystalline. This shows that submicron-sized particles can be obtained by this technique. The choice of the calcination temperature has a marked effect on the size of the particles and hence, particles of the desired size range can be obtained by choosing a suitable heating temperature.

(3) During the individual decomposition of barium citrate, $BaCO_3$ was obtained at 400 °C. Further decomposition of this carbonate requires a very high temperature ($\sim$ 1700 °C) for conversion to the oxide. The thermal decomposition of the mixture of Zn citrate and barium citrate, however, showed the formation of barium oxide at 1140 °C. In the presence of zinc oxide, therefore, barium oxide is obtained at a much lower temperature than that needed for the decomposition of barium citrate alone. This BaO obtained at 1140 °C is reactive and unstable, and is found to react with zinc oxide probably forming barium zincate.

(4) The thermal decomposition of calcium citrate resulted in the formation of CaO at 1150 °C while that of the mixture showed the formation of CaO at about 800 °C. It is probable that the calcium and zinc oxides obtained at the end of the thermal decomposition of the mixture react with

each other, forming a new compound. At this stage it is difficult to identify this compound exactly but it is most likely to be $CaZnO_2$ as the citrates of zinc and calcium were originally taken in 1 : 1 proportion.

(5) During the thermal decomposition of bismuth citrate, α-Bi_2O_3 was obtained as the end product at 350 °C while the decomposition of the mixture of zinc and bismuth citrates yielded the β-phase of Bi_2O_3.

(6) The liquid mix technique can be used to obtain reproducible mixtures of the oxides.

ACKNOWLEDGEMENT

A. Srivastava thanks the Council of Scientific and Industrial Research, New Delhi, for the award of a Senior Research Fellowship.

REFERENCES

1 M.P. Pechini, U.S. Patent 3,330,697 (1967).
2 C. Marcilly, P. Courty and B. Delmon, J. Am. Ceram. Soc., 83 (1970) 56.
3 M. Matsuoka, Jpn. J. Appl. Phys., 10 (1971) 736.
4 A. Srivastava, P. Singh, V.G. Gunjikar and C.I. Jose, Thermochim. Acta, 76 (1984) 249.
5 J. Mastowska, J. Therm. Anal., 29 (1984) 895.
6 A. Radecki and M. Wesolowski, Thermochim. Acta, 17 (1976) 217.
7 F. Smeets, U.S. Patent 3,586,715 (1966).
8 R.A. Nyquist and R.O. Kagel, in Infrared Spectra of Inorganic Molecules, Academic Press, London, 1971, p. 221.
9 N.T. McDevitt and W.L. Baun, Spectrochim. Acta, 20 (1964) 799.
10 R.A. Nyquist and R.O. Kagel, in Infrared Spectra of Inorganic Molecules, Academic Press, London, 1971, p. 79.
11 L.J. Bellamy, in Infrared Spectra of Complex Molecules, Wiley, New York, 1957, p. 34.
12 R.A. Nyquist and R.O. Kagel, in Infrared Spectra of Inorganic Molecules, Academic Press, London, 1971, p. 207.
13 C.D. Hodgmann, in Handbook of Chemistry and Physics, Chemical Rubber Publishing Co., Cleveland, OH, 1958, p. 538.
14 A. Srivastava, Ph.D. Thesis, 1985.